BioChip J. (2014) 8(1): 35-41
DOI 10.1007/s13206-014-8106-2

Original Article

Sensitivity response to coating material thickness for an optical resonant reflective biosensor based on a guided mode resonance filter

Bong Kyu Kim[1], Kyung-Hyun Kim[1], Jongcheol Hong[1], Wan-Joong Kim[1], Hyunsung Ko[1], Chul Huh[1], Gun Yong Sung[2], Won Ick Jang[1], Sun Hee Park[1] & Soo Jun Park[1]

Received: 18 December 2013 / Accepted: 18 February 2014 / Published online: 20 March 2014

Abstract Sensitivity is a very important parameter for biosensor applications. We have numerically and experimentally studied the sensitivity and linewidth responses of optical resonant reflective biosensors to the thickness of high refractive index materials coating the grating layer used to create a guided mode. Zero sensitivity, which may create serious problems in biosensors, is obtained when the coating material has a relatively low refractive index and a thin coating thickness (near the cutoff condition in which a high index layer is no longer capable of acting as a waveguide). The sensitivity and linewidth are greatly influenced by the thickness of the coating material. The thickness also has an optimal state, which is a very important factor for designing highly sensitive optical resonant reflective biosensors using a guided mode resonance filter.

Keywords: Biosensor, Optical resonance reflection biosensor, Guided mode reflection filter, Sensitivity, Nanostructure

Introduction

Biosensor development is driven by a continuous need for compact and rapid health monitoring within a broad area[1,2]. Among the many biosensors available, the optical biosensor is a very attractive item of research as it provides measurements for low biomarker and protein concentrations[3]. In particular, a guided mode resonance filter (GMRF)[4-9] is a promising device for use in biosensors. A GMRF uses a wavelength shift measurement scheme, which makes it possible to be mass produced, thus reducing the cost of biochip devices[10]. Optical resonant reflective biosensors (ORRBs) based on a GMRF can measure protein concentrations by observing the peak wavelength that is shifted by the interaction between a protein and its antibody[11-13]. The grating layer of a GMRF used in biosensor applications is thinly coated with a high refractive index material such as TiO_2 or SiN_x. These GMRF based sensors are compact and have high sensitivity with label-free detection. However, we have observed that the sensitivity of fabricated GMRFs was changed by the coating condition and the sensitivity was zero in special condition. Therefore, for detecting the early stages of a disease or screening other diseases, it is necessary to analyze the dependency of the thinly coating layer.

The coating layer is used to create a guided mode. As light is guided into the grating and coating layers, both layers affect the peak reflection wavelength that is determined by the guided mode's resonant condition. The peak wavelength and resonant condition can also be changed by the variance of the refractive index and the layer thickness of materials adjacent to the coating layer. The amount of peak wavelength shift is an important parameter because it is directly proportional to the sensitivity of an ORRB.

In reference 12, the sensitivity was numerically sim-

[1]Bio-medical IT Convergence Department, ETRI, Yusong-Gu, Daejeon 305-701, Korea
[2]Department of Materials Science & Engineering, College of Information & Electronic Engineering, Hallym University
Correspondence and requests for materials should be addressed to B.K. Kim (✉bongkim@etri.re.kr)

ulated and described by using the modal overlap in the detection zone. The predicted sensitivities were obtained for various grating step heights. In this work, we have numerically and experimentally studied the sensitivity dependency on the coating material thickness. The results show that sensitivity is greatly influenced by the coating thickness. In particular, when the coating thickness is too thin or too thick, the sensitivity is reduced, making it too low for biosensor applications. Therefore, to utilize an ORRB in biosensor applications or to fabricate an ORRB with high sensitivity, the optimal coating thickness of the GMRF should be determined. We have also studied the linewidth characteristics of the GMRF reflection spectrum for various coating material thicknesses, which is related to the sensor resolution of an ORRB. We have come to realize that a GMRF can be easily optimized by observing the shape of the reflection spectrum when minimizing the linewidth. This will be very useful for use in biosensor systems requiring high resolution.

Results and Discussion

Structure and fabrication of GMRF

Figure 1(a) depicts a schematic diagram of the fabricated GMRF with a sub-wavelength periodic structure, while Figure 1(b) shows its scanning electron microscope (SEM) imaging. The grating layer, made of polymer resin with a refractive index of n=1.5, had a periodic modulated structure and was fabricated on a SiO_2 substrate of n=1.482. The height (h_s) of the grating step was 160 nm, and the widths of the grating step and groove were 320 nm and 210 nm, respectively. Before immobilizing antibodies or bio-receptors, a high index coating material such as SiN_x and TiO_2 is coated onto the surface of the grating layer in order to create the guided-mode resonance in the GMRF. In this work, the SiN_x, with a refractive index n_c of approx. 2.0, was made up of crystalline Si nanodots embedded on an amorphous layer and coated with grating resin using plasma enhanced chemical vapor deposition (PECVD). The PECVD was operated at 13.56 MHz and 600 W with a process pressure of 0.9 Torr, and the SiN_x was deposited at 150°C using SiH_4/N_2 gas. During this processing step, the ratio of the thickness of the high index material coating at the top with that at the wall ($t_{hi} : w_{hi}$) was measured to be 1 : 0.8, as shown in Figure 1(b). The area of the fabricated grating layer was 0.5×0.5 mm^2.

Numerical and experimental analysis

As the light incident to the GMRF is guided in the grating and coating layers[4,5], and[14], the resonant condition of the guided mode is determined by the dimensions as well as the refractive indices of the coating and grating layers. In addition, the resonant condition is also changed by the variance of the refractive index and the layer thickness of materials adjacent to the coating layer. As target antigen molecules in the superstrate (solvent) are captured by antibodies or bio-receptors immobilized on the high index coating layer, the resonant condition is changed, and the peak wavelength of the reflection signal is shifted. The amount of wavelength shift depends on the high index coating thickness as well as on the refractive index of the target molecule. In order to analyze the dependency of the sensitivity on coating thickness t_c, we calculated the peak wavelengths for different refractive indices (n_s) of the target molecules. Here, we used GSolver[15] as a numerical grating analysis tool and considered only a normal incident TM-polarized wave of which the electric field direction is perpendicular to the grating lines. In this design, the TM-polarized wave was selected due to a narrower resonance linewidth compared to

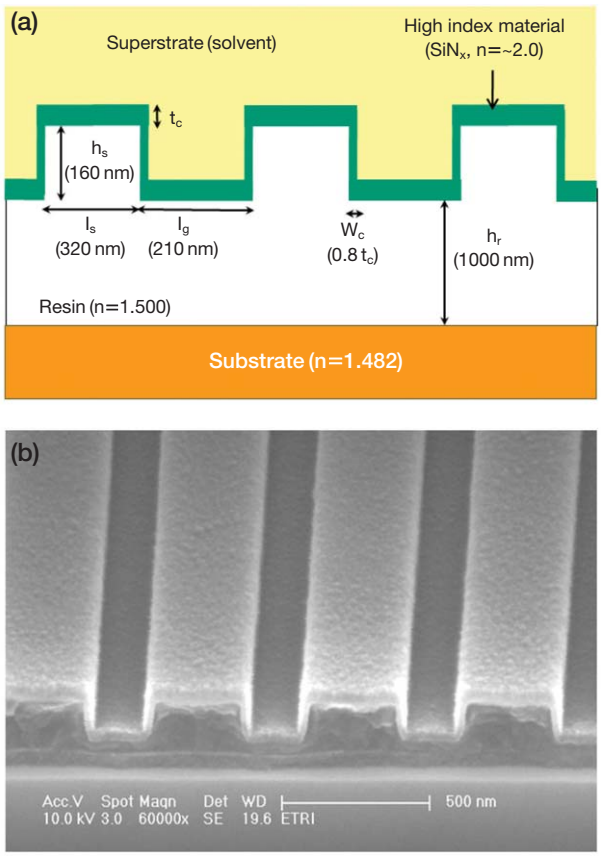

Figure 1. A cross section of the GMRF structure: (a) schematic diagram, and (b) SEM imaging.

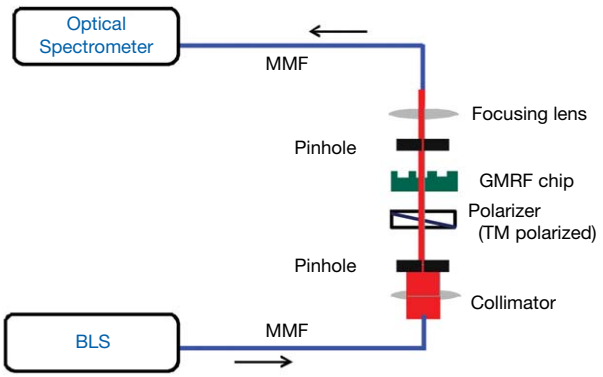

Figure 2. Experimental setup for measuring the peak wavelength and transmission spectrum of the fabricated GMRF. BLS: broadband light source, MMF: multimode fiber.

the TE-polarized wave[12]. The GMRF model without an immobilization layer of antibodies was considered for a simplified analysis. For analysis of the sensitivity, we calculated the bulk sensitivity coefficient (BSC) as introduced in[11] and[12]. The BSC was calculated using two peak wavelengths, which were obtained from the spectra for two different refractive indices (n_s) of the solvent.

We also performed an experimental analysis by observing the transmission spectrum of a GMRF. Figure 2 depicts the configuration of the experimental setup. A tungsten halogen source with a broadband spectral range of 200 to 2000 nm was used as a broadband light source (BLS). The transmitted light through multimode fiber (MMF) was collimated. The collimation beam was incident to the fabricated GMRF through a linear polarizer that is used to transmit TM-polarized light. The transmitted signal from the GMRF was inserted into an optical spectrometer (Andor, Shamrock SR-500i) with a wavelength resolution of 0.05 nm. As the spectrum shapes and peak wavelengths of the transmission and reflection spectra of the GMRF depend on the light incident angle to the GMRF[5,14], two pinholes with a diameter of 0.3 mm were inserted between the collimator and focusing lens to intercept divergent beams. The distance between the two pinholes was approx. 30 cm. Also, since we observed that the peak wavelength and linewidth of the transmission spectrum have minimum values when the incident angle of the TM polarized light is perpendicular to the surface of the GMRF, we adjusted the incident angle to minimize the peak wavelength value by tilting the GMRF.

For an analysis of the coating thickness dependency, we fabricated GMRF chips with various coating thicknesses. The coating thickness was controlled based on the deposition time during the coating process using the PECVD method. The GMRF chip used for the

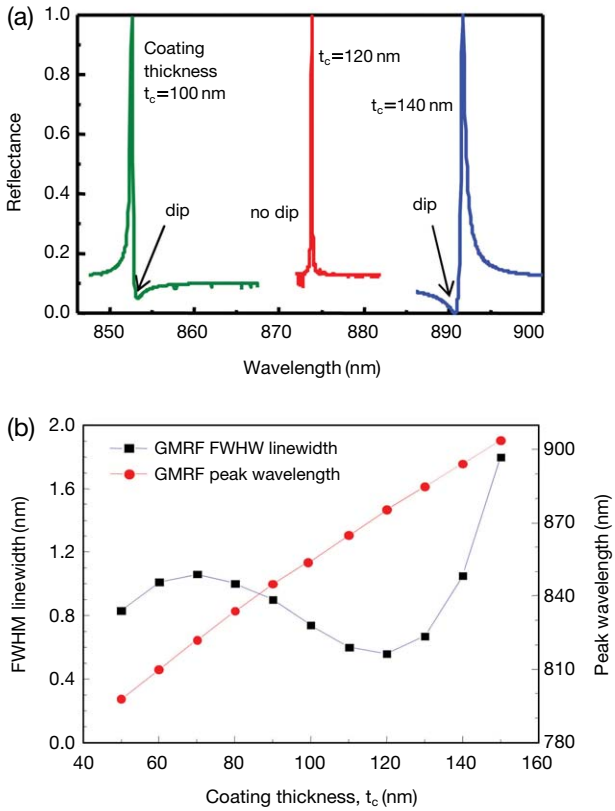

Figure 3. (a) The numerically obtained reflection spectra of the GMRF for coating thicknesses t_c of 100 nm, 120 nm, and 140 nm, and (b) peak wavelength and linewidth characteristics as a function of coating thickness t_c. The full wave half maximum (FWHM) linewidth was calculated from the reflection spectra.

sensitivity test was simultaneously fabricated with a sample chip in order to measure the coating thickness via an SEM during the same coating process. The fabricated GMRF chips had sharp resonant peak signals with FWHM linewidths of 1 to 2 nm. The BSC was calculated based on two peak wavelengths that were measured from the spectra for two different refractive indices (n_s) of the solvent, as described in the numerical analysis.

Sensitivity & bulk shift coefficient

Figure 3(a) depicts the simulation results for the reflection spectra of the GMRF using various coating thickness plotted from data calculated using a numerical grating analysis tool (GSolver)[15]. Here, the refractive index of superstrate n_s and the refractive index of high index coating material n_c were 1.33 and 2.1, respectively. As the coating thickness t_c increased, the peak wavelength increased and the spectrum shape as well as the linewidth changed. Figure 3(b) shows the simu-

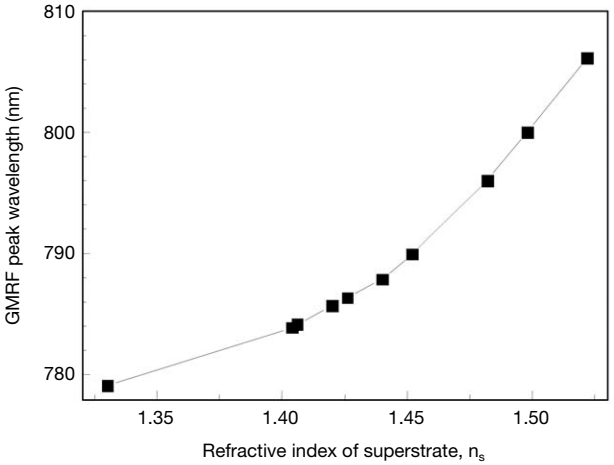

Figure 4. Experimental results of the relation of peak wavelength and refractive index n_s of superstrate at t_c=50 nm.

lation results of the peak wavelength and full-width half-maximum (FWHM) linewidth as a function of coating thickness. The peak wavelength increased continuously as the coating thickness increased. However, the linewidth response to the coating thickness was different with the peak wavelength response, and the linewidth was minimized at a 120 nm coating thickness in the 50 to 150 nm thickness range.

When the linewidth was minimized, the shape of the reflection spectrum was symmetric, as illustrated in Figure 3(a). On the other hand, the reflection spectra are asymmetrical and there is a dip in spectrum for the other thicknesses. These asymmetric spectra and dips have been reported in many previous works[12-14]. However, a relationship between shape/dip and linewidth has not been reported. The dip was located on the right side of the peak wavelength when the coating layer thickness was thinner than 120 nm, which provides a minimum linewidth. On the other hand, the dip was positioned at the left side when the thickness was more than 120 nm. Therefore, it is easy to minimize the linewidth of the GMRF by observing the dip position or symmetric shape. This will be very useful for systems requiring a GMRF with narrow linewidth for high resolution biosensor applications.

To analyze the sensitivity of the ORRB, we obtained the bulk shift coefficient (BSC) from the peak wavelength shift, as introduced in[11] and[12]. To obtain the BSC, we measured the peak wavelength for various superstrate indices n_s using various index matching oils and chemical solutions used as a superstrate. The peak wavelength was measured from the spectrum obtained using an optical spectrometer with a 0.05 nm wavelength resolution.

Figure 4 shows the measured peak wavelength as a

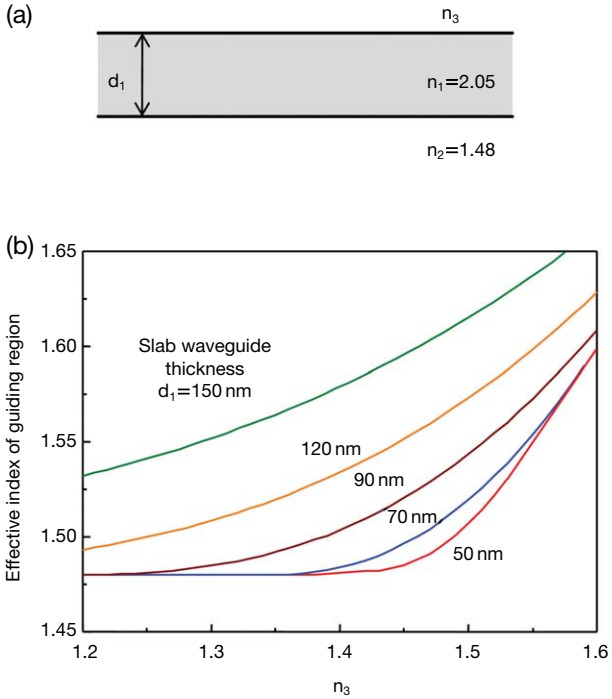

Figure 5. (a) Slab waveguide structure, and (b) the effective index of the guided mode for various thicknesses of d_1.

function of the refractive index n_s of the superstrate when a high index material of SiN_x with a refractive index of n_c=2.0 was used to coat the grating layer. The measured peak wavelengths based on a coating thickness t_c of 50 nm are depicted in Figure 4. The peak wavelength continuously increases as n_s is increased. However, the slope, which is the peak wavelength shift per refractive index unit of the superstrate, at a high n_s area of above 1.5 is about 3.5 times greater than the slope at the region of a low n_s, which has an area of 1.3 to 1.4. The slope also increases as n_s is increased. We predicted that the BSC of the GMRF, which corresponds to the ORRB sensitivity, will decrease as the refractive index of superstrate n_s decreases. Because a superstrate with a refractive index of 1.3 to 1.4 is generally utilized for biosensor applications, an improvement in slope is needed.

A GMRF has a sub-wavelength grating structure. Therefore, normal incident light entering the GMRF propagates along the grating layer, including the high refractive index coating layer[8,9]; the grating layer plays the role of a waveguide and reflects phase matched light[5,14]. The resonant reflection (phase matching) condition depends on the grating period and effective index of the grating layer. As a GMRF structure without a grating form is similar to a slab waveguide[9], we have calculated the effective index characteristics for a guid-

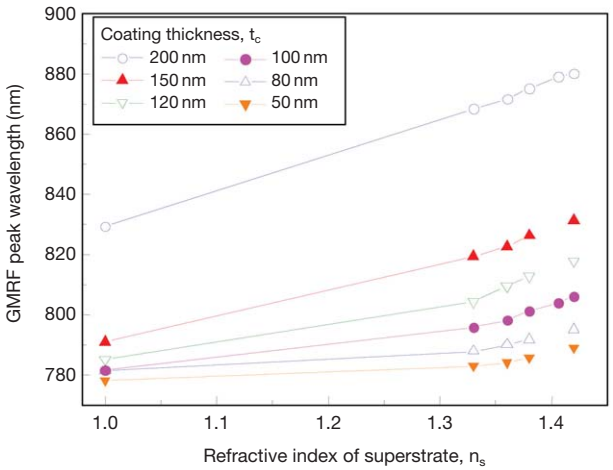

Figure 6. Experimental results of the relation between peak wavelength and refractive index n_s of a superstrate for various coating thicknesses of t_c.

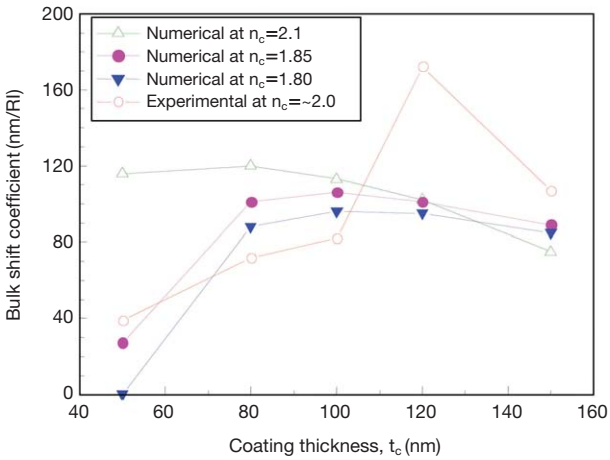

Figure 7. Experimental and numerical results of the bulk shift coefficient (BSC) as a function of coating thickness t_c for various coating refractive indices n_c when the refractive index of the superstrate n_s is 1.33.

ed mode in a three-layer dielectric slab[16], depicted in Figure 5(a), in order to simply analyze the reason for the variation in peak wavelength characteristics of the GMRF. The slopes, which indicate the effective index variation per n_3 unit, were almost zero at a low n_3 region below approx. 1.4 for d_1 thicknesses of 50 and 70 nm as shown in Figure 5(b). However, the effective index and slopes continuously increase as n_3 is increased at the region of $n_3 > 1.4$. This effective index variation response in a slab waveguide is similar to the peak wavelength characteristics shown in Figure 4, and we assume that the coating thickness dependency is from the guided mode characteristics in a slab waveguide.

For a further analysis of the peak wavelength response, the peak wavelengths were measured for various coating thicknesses. Figure 6 illustrates the measured peak wavelength responses for these various thicknesses. The peak wavelengths at a high n_s increase more steeply as n_s increases in all cases compared to a low n_s region, which is similar to the response observed in Figure 4. However, as the coating layer of the SiN_x thickens, the difference between the rising slopes at the low and high n_s regions decrease: the peak wavelength linearly increases in a more relative fashion compared with the thin coating thickness. This shows that the dependency of the BSC, or the sensitivity of the refractive index of the superstrate, is reduced as the coating thickness increases. In addition, the rising slope of the peak wavelength shift increases as the thickness is increased; that is, the sensitivity increases dependent upon the thickness.

For an accurate analysis of ORRB sensitivity, we obtained the BSC of the GMRF from the measured and simulated peak wavelengths. The experimental values of the BSC were obtained from the measured peak wavelengths when deionized water with n_s=1.33, and acetone with n_s=1.36, were used as superstrates. The experimental BSC was calculated by dividing the difference between the two measured peak wavelengths by the difference (0.03) of the refractive indices of the applied superstrates. The obtained experimental BSC ($BSC_{exp} \equiv (\lambda_{n=1.36} - \lambda_{n=1.33})/(n_{1.36} - n_{1.33})$) as a function of the coating thickness was plotted as shown in Figure 7.

We have also numerically obtained the BSC from the peak wavelength simulated using an analysis tool, GSolver. Here, we considered two different indices n_s of 1.330 and 1.331 as the superstrates, and the BSC was obtained from the difference between the two simulated peak wavelengths. The numerically obtained BSCs of the GMRFs are also depicted in Figure 7. The BSC variation characteristics according to the change in coating thickness have some different responses for the various coating indices of n_c. For a thin thickness, the BSC values of GMRFs with low coating indices of n_c=1.8 and 1.85 vary greatly compared with a high coating index of n_c=2.1. The values were rapidly reduced by thinning the coating thickness, and a BSC of zero was obtained when the coating material included n_c=1.8 coats with a thickness of 50 nm. The dependence of the BSC on the thickness is reduced as the coating index increases; this result shows that the sensitivity of the ORRB is strongly dependent upon the index and the thickness of the coating material. The experimentally obtained BSC had strong dependence on the coating thickness; this result is similar to the numerically obtained BSC results for a refractive index

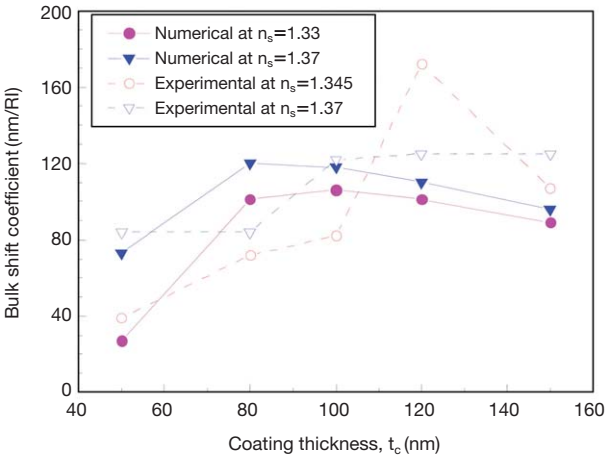

Figure 8. The experimental and numerical results of the bulk shift coefficient (BSC) as a function of the coating thickness t_c for two different superstrate indices of n_s=1.33 and n_s= 1.37. Here the refractive index n_c of a high index coating material was 1.85 in the numerical simulation.

of n_c=1.85, although the measured refractive index of the SiN_x used as a coating material was 2.0 at a wavelength of 633 nm.

We also obtained the BSCs for another superstrate that has a different refractive index. The triangular diagrams in Figure 8 show the experimentally and numerically obtained BSCs as a function of coating thickness t_c for the different superstrates; in order to analyze more characteristics, we set n_s=1.37. The coating material with a refractive index n_c of 1.85 was used in the numerical simulation. The BSC values were larger compared to the value for a low n_s of 1.33; however, the curves are similar to the curves described in Figure 7, and the maximum value also exists in the considered region. This result shows that the coating thickness has a great influence on the sensitivity, and that there is an optimal thickness dependent on the refractive index of not only the coating material but also the superstrates.

Conclusions

We experimentally measured and numerically calculated the peak wavelength and FWHM linewidth of a GMRF for a sensitivity analysis of an ORRB. We know that the GMRF characteristics including sensitivity are greatly influenced by the thickness of the high index material used for setting up the guided mode. A low refractive index and thin coating material reduce the sensitivity to as low as zero; this makes it possible for serious problems to be generated in an ORRB system. Therefore, the thickness and refractive index of the high index coating material are very important factors in designing a biosensor with high sensitivity in ORRB systems.

Materials and Methods

Numerical analysis was performed by using the rigorous diffraction grating analysis tool, GSolver V5.1 (Grating Solver Development Co.). The used polarization axis for numerical and experimental analysis was TM mode.

Acknowledgements This work was partially supported by Industrial strategic technology development program, 10042581 funded by the Ministry of Trade, Industry & Energy (MOTIE) in Korea and internal research program, 14RC1200 funded by ETRI.

References

1. Bosch, M.E., Sanchez, A.J.R, Rojas, F.S. & Ojeda, C.B. Recent development in optical fiber biosensors. *Sensors* **7**, 797-859 (2007).
2. Lim, S.C. *et al*. Fabrication and characterization of an OTFT-based biosensor using a biotinylated F8T2 polymer. *ETRI J*. **31**, 647-652 (2009).
3. Tubb, A.J.C., Payne, F.P., Millington, R.B. & Lowe, C.R. Single-mode optical fibre surface plasma wave chemical sensor. *Sensors and Actuators B* **41**, 71-79 (1997).
4. Magnusson, R. & Wang, S.S. New principle for optical filters, *Appl. Phys. Lett*. **61**, 1022-1024 (1992).
5. Wang, S.S. & Magnusson, R. Theory and applications of guided-mode resonance filter. *Appl. Opt*. **32**, 2606-2613 (1993).
6. Mashev, L. & Popov, E. Zero order anomaly of dielectric coated gratings. *Opt. Communications* **55**, 377-379 (1985).
7. Boye, R.R. & Kostuk, R.K. Investigation of the effect of finite grating size on the performance of guided-mode resonance filter. *Appl. Opt*. **39**, 3649-3653 (2000).
8. Song, H.Y., Kim, S. & Magnusson, R. Tunable guided-mode resonances in coupled grating. *Opt. Express* **17**, 23544-23555 (2009).
9. Ngo, Q.M., Kim, S., Song, S.H. & Magnusson, R. Optical bistable devices based on guided-mode resonance in slab waveguide grating. *Opt. Express* **17**, 23459-23467 (2009).
10. Chang, A.S.P. *et al*. Tunable liquid crystal-resonant grating filter fabricated by nanoimprint lithography. *IEEE Photonics Technology Letters* **19**, 1457-1459 (2007).
11. Wawro, D.D., Tibuleac, S., Magnusson, R. & Liu, H.

Optical fiber endface biosensor based on resonance in dielectric waveguide gratings. *Proc. of SPIE* **3911**, 86-94 (2000).
12. Block, I.D., Ganesh, N., Meng. L. & Cunningham, B.T. A sensitivity model for predicting photonics crystal biosensor performance. *IEEE Sensors Journal* **8**, 274-280 (2008).
13. Hong, J. *et al*. Prediction of the limit of detection of an optical resonant reflection biosensor. *Opt. Express* **15**, 8972-8978 (2007).
14. Magnusson, R. *et al*. Photonic devices enabled by waveguide-mode resonance effects in periodically modulated films. *Proc. SPIE* **5225**, 20-34 (2003).
15. Gsolver© V5.1 Diffraction Grating Analysis Program. http://www.gsolver.com/brochureV51.pdf.
16. Adams, M.J. An introduction to optical waveguides (John Wiley and Sons Ltd., New York, pp. 20-28, 1981).